Title	Carbon nanotube parametric electron pump: A molecular device
Author(s)	Wei, Y; Wang, J; Guo, H; Roland, C
Citation	Physical Review B (Condensed Matter and Materials Physics), 2001, v. 64 n. 11, p. 115321:1-4
Issued Date	2001
URL	http://hdl.handle.net/10722/43346
Rights	Creative Commons: Attribution 3.0 Hong Kong License

Carbon nanotube parametric electron pump: A molecular device

Yadong Wei,[1] Jian Wang,[1] Hong Guo,[2] and Christopher Roland[3]
[1]*Department of Physics, University of Hong Kong, Pokfulam Road, Hong Kong, China*
[2]*Centre for the Physics of Materials and Department of Physics, McGill University, Montreal, PQ, Canada H3A 2T8*
[3]*Department of Physics, North Carolina State University, Raleigh, North Carolina 27695*
(Received 13 November 2000; revised manuscript received 11 June 2001; published 31 August 2001)

We have analyzed the device properties of a single-wall metallic carbon nanotube operated as a parametric electron pump. It is found that a dc current can be pumped out from this molecular device by a cyclic variation of two gate voltages near the nanotube, in the absence of any bias voltage. Due to the particular electronic properties of the nanotube, the pumped current is found to show a remarkable parity effect near the resonant levels, with a rather sensitive dependence on the control parameters of the device such as deformation strength, the amplitude and the phase difference of the gate voltage.

DOI: 10.1103/PhysRevB.64.115321 PACS number(s): 72.80.Rj, 73.61.Wp, 73.23.Ad

Since their original discovery, carbon nanotubes (CNT's) have been the subject of intensive experimental and theoretical investigations. So far many interesting nanotube devices have been explored, including single-electron transistor,[1] tunneling-magnetoresistance device,[2] electromechanical switch[3]; CNT diodes,[4] intramolecular junctions,[5] CNT quantum wires,[6,7] CNT-superconductor hybrid systems,[8] heterostructure,[9] and CNT rings[10] and crosses.[11] In this paper, we propose and investigate the properties of a nanotube-based parametric electron pump, a molecular device by which a dc electric current is delivered to the outside world at zero bias voltage via a cyclic deformation of two or more device parameters.[12,13]

Classical pumps have been fabricated a long time ago based on the Coulomb blockade effects.[14,15] More recently, quantum-dot-based quantum pumps were investigated,[16] in which a dc signal was delivered by cyclically deforming the shape of the quantum dot using two gates that were capacitively coupled to the dot. The output signal was found to vary with the phase difference ϕ_0 between the two gate voltages, and to be antisymmetric about $\phi_0=\pi$. Because such an output can be delivered without bias, this interesting device has been the subject of several theoretical investigations.[17–20] Due to the peculiar electronic properties of CNT,[5,2,6–8,21,22] CNT-based parametric electron pumps are expected to behave as a prototypical nanometer-scale molecular device. Our main results show that this is indeed true, with the pumped dc current being sensitive to the electronic levels of the CNT. An antisymmetric pumped signal is predicted near the many doubly degenerate levels of the finite-length CNT for a wide range of energies, along with a nonsinusoidal dependence on the phase difference ϕ_0 on the external pumping force. Finally, we predict a ''phase diagram'' for the parametric pumping operation of the CNT device.

The CNT pump we consider (see the left inset of Fig. 2) consists of a finite-sized metallic CNT connected to two electrodes. It is operated by applying cyclic, time-dependent gate voltages to the two metallic gates, which are capacitively coupled to the CNT. Due to these gate voltages, two potential perturbations, which vary cyclically, are established along the length of the tube. For the pump to work, we assume that the two pumping forces have a definite phase difference ϕ_0. For simplicity, the CNT is modeled with the nearest-neighbor π-orbital tight-binding model with bond potential $V_{pp\pi}=-2.75$ eV for the carbon atoms. This model is known to give a reasonable, qualitative description of the electronic and transport properties of carbon nanotubes.[23,24] Although model analysis of parametric pumps have been carried out before within the context of scattering-matrix theory,[18,20] molecular systems such as CNT's differ in that the atomic structure plays an important role in determining the output signatures. To investigate, we therefore used a nonequilibrium Green's function approach.[25,26] We further assume that the CNT is well contacted by the electrodes and that the temperatures are such that both the Coulomb blockade effects and electron-electron interactions may be neglected.

In the pumping process, we use $\{X(t)\}$ to describe a set of external pumping forces that are functions of time t. In the adiabatic approximation, the current flowing through electrode α due to variations of driving forces X_1 and X_2, in one period of time τ, is given by[18]

$$I_\alpha \equiv \int_0^\tau I_\alpha(t)dt = \frac{q\omega}{2\pi}\int_0^\tau dt\left[\frac{dN_\alpha}{dX_1}\frac{dX_1}{dt}+\frac{dN_\alpha}{dX_2}\frac{dX_2}{dt}\right], \quad (1)$$

where the quantity dN_α/dX is the partial density of states (DOS), called the injectivity, of lead α (Ref. 27)

$$\frac{dN_\alpha}{dX_j}=-\int\frac{dE}{2\pi}\left(-\frac{\partial f}{\partial E}\right)\mathrm{Tr}[G^r\Gamma_\alpha G^a\Delta_j], \quad (2)$$

which describes the number of charged carriers entering lead α due to the change of parameter X_j. Here the retarded Green's function is given by

$$G^r(E,\{X\})=\frac{1}{E-H-V_{pp}-\Sigma^r}, \quad (3)$$

where $\Sigma^r\equiv\Sigma_L^r+\Sigma_R^r$ is the total self-energy due to coupling to the device electrodes, and $\Gamma_\alpha=-2\,\mathrm{Im}[\Sigma_\alpha^r]$ is the linewidth function. In Eq. (3), V_{pp} is a diagonal matrix describing the variation of the CNT potential landscape due to the external pumping force X. In this work we choose the two

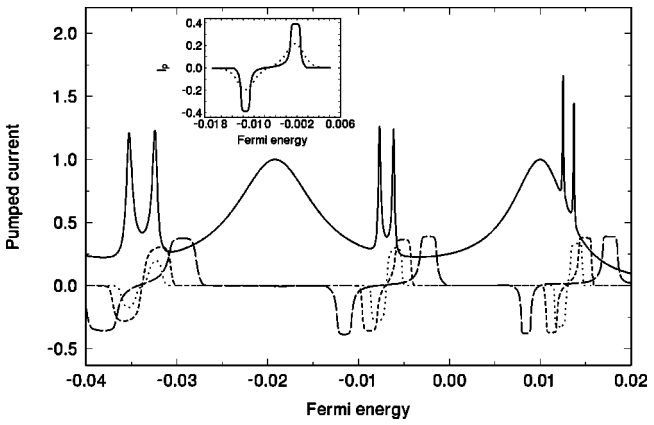

FIG. 1. The transmission coefficient (solid line), the pumped current versus E_F for different pumping amplitudes $V_p=0.0014$ (dotted line), 0.0027 (short-dashed line), and 0.0068 (long-dashed line). Inset: the pumped current versus E_F with $T=0$ (solid line) and $T=10$ K (dotted line) with $V_p=0.0068$. The other parameters are $V_0=2.72$ and $\phi_0=\pi/2$.

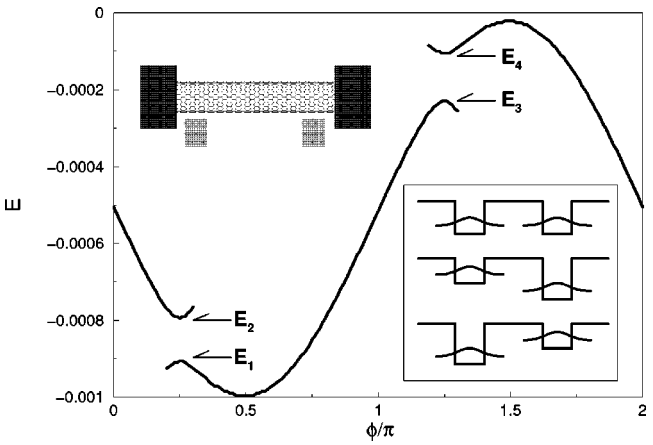

FIG. 2. The location of the peak of injectivity dN_1/dX_1 versus the phase ϕ/π. Left inset: a schematic plot of the molecular device. Right inset: the localized wave functions in the wells.

external forces to be $X_1(t)\equiv V_1(t)=-V_{10}-V_{1p}\sin(\omega t)$ and $X_2(t)\equiv V_2(t)=-V_{20}-V_{2p}\sin(\omega t+\phi_0)$. The potential due to the gates can therefore be written as $V_{pp}=V_1\Delta_1+V_2\Delta_2$, where Δ_i is the potential profile function.

We now apply Eq. (1) to calculate the current for the CNT parametric pump. In particular, we consider a (5,5) armchair CNT with 200 unit cells of carbon atoms (total 4000 atoms). In this work we specifically consider situations where the nanotube is well contacted and therefore transport is not in the Coulomb blockade regime. The two metallic gates that provide the driving force are located near the two ends of the finite CNT between $0.1L$ to $0.3L$, and between $0.7L$ to $0.9L$, where L is the length of the CNT (each gate has a size of 40 unit cells). To simplify the numerics, we mimic the gate effects by simply adding the potential V_{pp} to the CNT where the profile function Δ_i is set to be unity for the gate region, and zero otherwise. A more-accurate study requires a numerical solution of the Poisson equation with the gates providing the appropriate boundary conditions. However, a simple potential shift is expected to be adequate for a semiquantitative study. We have also applied the wide bandlimit for the self-energy[25,28] and, without losing generality, assumed $V_{10}=V_{20}=V_0$ and $V_{1p}=V_{2p}=V_p$. If the pumping is asymmetric, the transmission coefficient and hence pumped current will be suppressed. The unit of the pumped current I_p is fixed by the pumping frequency. When frequency $\omega=100$ MHz, which is close to the frequency used in Ref. 16, $I_p\sim 10^{-11}$ A. Finally, the energy scale such as Fermi energy and gate voltages is measured in eV.

Figure 1 shows the pumped current I_p versus the Fermi energy E_F for different pumping amplitudes V_p, with $V_0=2.72$ (Ref. 29) and $\phi_0=\pi/2$ at zero temperature. For comparison, we also plot the static transmission coefficient of the CNT device at zero pumping force $V_p=0$ (solid line). Several interesting observations are in order. First, the transmission function shows a resonance behavior indicated by the many sharp and broad peaks. We have confirmed that the sharp peaks occur at energies where there are very large-scattering total DOS, while the broad peaks are at energies characterized by smaller total DOS. This behavior is consistent with a resonant transmission due to a coupling of the CNT to the external electrodes. The sharp transmission peaks are usually grouped in pairs, which is a consequence of the finite-sized CNT energy spectrum that has many doubly degenerate levels.[30] When the CNT is in contact with the external electrodes, these degenerate levels split, resulting in the resonance pairs. Second, due to the resonance transmission, the pumped current I_p has a large value near energies where the sharp resonant transmission peaks occur, while I_p vanishes away from these peaks. This is because I_p is directly proportional to the scattering DOS. Therefore, even at energies where the transmission has broad resonances such as at $E\approx -0.0204$, I_p does not show any peak due to the small DOS there. Third, another striking aspect is that the pumped current peaks have opposite sign for each transmission pair peaks, and the width of the current peaks is close to the distance between the transmission peaks. Therefore, the CNT pump has the property that the DC current can flow out of the device from either electrodes by a slight change of electron energy. Finally, as the pumping force amplitude V_p increases, the current peak height increases and its position is shifted away from the original transmission peak.

To understand this behavior, we note that in the symmetric pumping case that we consider, the pumped current in the left lead at time t is given by,

$$I_1(t)\sim \frac{dN_1}{dX_1}\cos\omega t-\frac{dN_1}{dX_2}\sin\omega t. \tag{4}$$

As will be discussed later, dN_1/dX_1 is much larger than dN_1/dX_2 (numerical results confirm this). Therefore, the pumped current I_1 is mainly determined by dN_1/dX_1, which shows sharp peaks near the resonant levels. We find that during a pumping cycle labeled by $\phi=\omega t$, dN_1/dX_1 has one or two very sharp peaks depending on the configuration of the pumping system. This is plotted in Fig. 2. Let us first examine Fig. 2 at a fixed ϕ. Since the pumping potential $V_1=V_0+V_p\sin\phi$ and $V_2=V_0+V_p\cos\phi$, during the pump-

ing cycle the system is always asymmetric (i.e., $V_1 \neq V_2$) except at $\phi=\pi/4$ and $5\pi/4$. These two special points correspond to the case in which the bands of both wells are shifted up and down by $(\sqrt{2}/2)V_p$. At $\phi=\pi/4$ (or $5\pi/4$), we see two large peaks at $E_1=-0.0122$ (or $E_3=-0.0027$) and $E_2=-0.0109$ (or $E_4=-0.0014$) corresponding to two resonant levels in the transmission curve. When $\phi<\pi/4$ or $\phi>5\pi/4$, the left well is higher than that of the right. We find that the injectivity dN_1/dX_1 for the lower resonant level diminishes very quickly, while that of the upper resonant level remains more or less the same. When the right well is lower for $\pi/4<\phi<5\pi/4$, we can only see the injectivity of the lower resonant level instead. Hence, Fig. 2 is actually a trace of the injectivity of the two resonant levels for the different system configurations.[31] Physically, Fig. 2 can be understood as follows. The system has two resonant levels in the energy range of $[-0.014,0]$ so that one observes two transmission peaks when $V_p=0$. These two resonant states Ψ_i $(i=u,l)$ can be expanded approximately by ψ_L and ψ_R, which are localized near the two potential wells, respectively (see the right inset of Fig. 2): $\Psi_i \sim \alpha_i\psi_L \pm \beta_i\psi_R$. Near a resonant level E_0, the injectivity of lead α (with $\alpha=L,R$) can be written approximately as the Breit-Wigner form[32]: $\Gamma_\alpha/[(E-E_0)^2+\Gamma^2/4]$ where Γ_α is the decay width into the lead α. So the injectivity of left lead is dominated by Γ_L. When $V_p=0$ the system is symmetric, we have $\alpha_i=\beta_i=\sqrt{2}/2$. The electron wave function is now extended into the two wells and the electron has an equal probability of escaping from either leads. Hence Γ_L for upper and lower resonant levels are approximately the same. When the pumping is turned on, then Ψ_i will not have equal weight on $\psi_{L/R}$ and the electron will tend to localize in one of the wells. For instance, for $\phi<\pi/4$ or $\phi>5\pi/4$, the band bottom of the left well is higher. For the upper level Ψ_u, we have $\alpha_u>\beta_u$, i.e., the electron on the upper level E_u will spend more time in the left well whereas for the lower level E_l we have $\alpha_l<\beta_l$ and so that electron will dwell longer in the right well. As a result, $\Gamma_L(E_u)\gg\Gamma_L(E_l)$ and the electron coming from the left has larger injectivity for the upper level than the lower one. This explains why dN_1/dX_1 is much larger for the upper level than the lower one (not shown in Fig. 2 since it is very small). For $\pi/4<\phi<5\pi/4$, the resonant levels across, i.e., the level localized in the left well now becomes the lower level instead of upper one. Similar discussion leads to the conclusion that $\Gamma_L(E_l)\gg\Gamma_L(E_u)$. In other words, the electron localized in the left well always has larger injectivity for the left lead regardless whether it is on the upper level or lower one. Since the physics is dominated by the left well for the injectivity of lead 1, we conclude that dN_1/dX_1 is much larger than dN_1/dX_2. Hence, Fig. 2 serves as a ''phase diagram'' of our molecular device and the pumped current can be found directly from Fig. 2.

To obtain the pumped current for a fixed Fermi energy, one should accumulate dN_1/dX_1 through the pumping cycle with weighting factor $\cos\phi$ [see Eq. (4)]. When $E_F>0$ or $E_F<-0.014$, there is no peak in Fig. 2 for dN_1/dX_1 and the pumping current is negligible as a result. For E_F between E_1 and E_2, there is only one peak in the second quadrant for ϕ that gives a negative current due to the weighting factor $\cos\phi$. Similarly, for E_F between E_3 and E_4, there is only one peak in the fourth quadrant for ϕ resulting in a positive current. For the other Fermi energies E_F in Fig. 2, there are two peaks for dN_1/dX_1 with comparable amplitudes located at ϕ and $\pi-\phi$, respectively. Since $\cos\phi=-\cos(\pi-\phi)$, these two contributions cancel each other and the pumped current is negligible. From the above discussion, we see that the energy range of the nonvanishing pumped current is determined by the two resonant levels E_1 and E_2 (or E_3 and E_4). To further support this picture, we look at transmission curve. Figure 3 shows the shifting of the transmission curve as we increase or decrease the bottom of the well by $\sqrt{2}/2V_p$. We see that as the bottom of the well increases, the pair of resonant levels move downward while keeping the resonant peak distance more or less the same, and vice versa. Looking at Fig. 2, at $\phi=\pi/4$, we have two peaks exactly corresponding to the two resonant peaks in Fig. 3. Finally Fig. 3 shows that the position and the width of the pumping current are directly determined by the shifting of the resonant transmission peaks. We have done similar calculations for different system parameters including the case of zigzag nanotubes [see, for example, the right inset of Fig. 3 for I_p versus E_F for a (9,0) nanotube] and verified that the main physical picture is unchanged.

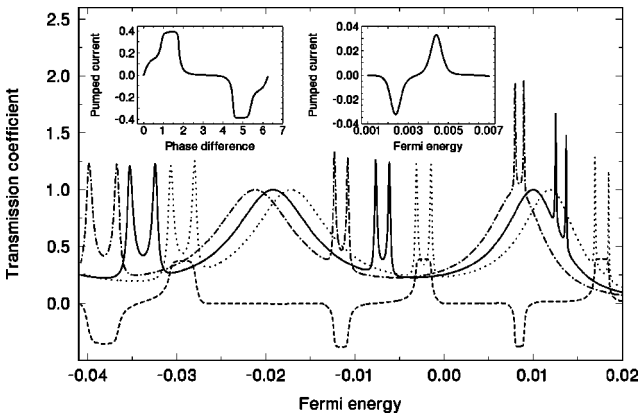

FIG. 3. The transmission coefficient and the pumped current versus E_F with $V_0=2.72$ and $V_p=0.0068$. Here three transmission coefficients are obtained by setting the bottom of the well to be V_0 (solid line), $V_0+\cos(\pi/4)V_p$ (dotted line), and $V_0-\cos(\pi/4)V_p$ (dash-dotted line). Left inset: I_p versus phase difference ϕ_0 for $V_0=2.72$, $V_p=0.0068$, and $E_F=-0.0019$. Right inset: I_p versus E_F for a (9,0) nanotube of 100 layers (total 3600 atoms) with $V_0=2.72$, $V_p=0.0041$, and $\phi_0=\pi/2$.

The left inset of Fig. 3 depicts the pumped current as a function of the phase difference ϕ_0. It shows that the pumped current is antisymmetric about $\phi_0=\pi$, consistent with the experiments of Ref. 16. Experimentally, for an open dot with a small DOS, it is observed[16] that the pumping signal is a sinusoidal function of the phase difference for small and intermediate pumping amplitudes. For strong pumping, the signal starts to show nonsinusoidal behavior. For our case, the nonsinusoidal behavior manifests itself via the resonant tunneling behavior. Note that the asymmetry of

pumped current around $\phi_0 = \pi$ can be destroyed by other effects such as the finite-frequency effect that is not considered here. Finally, we have studied the influence of higher temperatures to the pumped current. As the temperature is increased, the peaks in the pumping curve decrease gradually, as shown in the inset of Fig. 1 for I_p versus E_F at 10 K. This is expected since a finite temperature tends to smear out the quantum resonances, and the pumped current peak is a direct result of resonant tunneling.

In summary, we have studied the parametric pumping of a finite-carbon nanotube using a nonequilibrium Green's function theory. As the Fermi energy is varied, the pumped current is found to oscillate in a regular fashion as a result of competition of resonant levels. Because of the resonant nature of the pumping, the pumped current shows nonsinusoidal dependence on the phase difference of the pumping parameters, consistent with the experimental findings.

We gratefully acknowledge support by a RGC grant from the SAR Government of Hong Kong under Grant No. HKU 7215/99P. H.G. was supported by NSERC of Canada and FCAR of Québec. C.R. was supported by ONR and NASA. We thank the Computer Center of the University of Hong Kong for computational facilities.

[1] M. Bockrath *et al.*, Science **275**, 1922 (1997).
[2] K. Tsukagoshi *et al.*, Nature (London) **401**, 572 (1999).
[3] L. Liu *et al.*, Phys. Rev. Lett. **84**, 4950 (2000).
[4] R.D. Antonov and A.T. Johnson, Phys. Rev. Lett. **83**, 3274 (1999).
[5] Z. Yao *et al.*, Nature (London) **402**, 273 (1999).
[6] S.J. Tans *et al.*, Nature (London) **386**, 174 (1997).
[7] S. Frank *et al.*, Science **280**, 1744 (1998).
[8] A.F. Morpurgo *et al.*, Science **286**, 263 (1999).
[9] Y. Zhang *et al.*, Science **285**, 1719 (1999).
[10] H.R. Shea *et al.*, Phys. Rev. Lett. **84**, 4441 (2000).
[11] M.S. Fuhrer *et al.*, Science **288**, 494 (2000).
[12] D.J. Thouless, Phys. Rev. B **27**, 6083 (1983).
[13] Q. Niu, Phys. Rev. Lett. **64**, 1812 (1990).
[14] L.P. Kouwenhoven *et al.*, Phys. Rev. Lett. **67**, 1626 (1991).
[15] H. Pothier *et al.*, Europhys. Lett. **17**, 249 (1992).
[16] M. Switkes *et al.*, Science **283**, 1905 (1999).
[17] B. Spivak *et al.*, Phys. Rev. B **51**, 13 226 (1995).
[18] P.W. Brouwer, Phys. Rev. B **58**, R10 135 (1998).
[19] F. Zhou *et al.*, Phys. Rev. Lett. **82**, 608 (1999).
[20] Y.D. Wei *et al.*, Phys. Rev. B **62**, 9947 (2000).
[21] D.H. Cobden *et al.*, Phys. Rev. Lett. **81**, 681 (1998).
[22] H. Mehrez *et al.*, Phys. Rev. Lett. **84**, 2682 (2000).
[23] X. Blase *et al.*, Phys. Rev. Lett. **72**, 1878 (1994); Y.A. Krotov *et al.*, *ibid.* **78**, 4245 (1997); L. Chico *et al.*, *ibid.* **76**, 971 (1996); V.H. Crespi *et al.*, *ibid.* **79**, 2093 (1997); L. Chico *et al.*, *ibid.* **81**, 1278 (1996); L. Chico *et al.*, Phys. Rev. B **54**, 2600 (1996).
[24] M. Buongiorno Nardelli, Phys. Rev. B **60**, 7828 (1999).
[25] A.P. Jauho *et al.*, Phys. Rev. B **50**, 5528 (1994).
[26] B.G. Wang *et al.*, Phys. Rev. Lett. **82**, 398 (1999); J. Appl. Phys. **86**, 5094 (1999).
[27] M. Büttiker and T. Christen, in *Quantum Transport in Semiconductor Submicron Structures*, edited by B. Kramer (Kluwer Academic, Dordrecht, 1996), pp 263.
[28] We consider situations where the nanotube is well contacted by the electrode and applying the wide bandlimit by fixing $\Gamma_\alpha = 3.4$ eV to make the device transparent in the absence of gate voltage.
[29] We have checked that there is no significant change in physics when the gate voltage V_0 is reduced from 2.7 V to 1.3 V within our model.
[30] There are two transmission channels for the (5,5) metallic nanotube at the Fermi energy.
[31] When the system is asymmetric, one of the resonant levels has very large injectivity dN_1/dX_1 while the other level (not shown in Fig. 2) it is very small.
[32] M. Büttiker *et al.*, Z. Phys. B: Condens. Matter **94**, 133 (1994).